


# An effective anti-oxidized strategy for ultra-narrow band absorber as plasmonic sensor

Yulian Li<sup>1</sup>  · Bowen An<sup>1</sup> · Shengming Jiang<sup>1</sup> · Jun Gao<sup>1</sup> · Xuejia Lu<sup>1</sup>

Received: 17 August 2016 / Accepted: 1 November 2016 / Published online: 10 November 2016  
© Springer Science+Business Media New York 2016

**Abstract** An effective strategy to avoid the Ag oxidized problem of the ultra-narrow band grating absorbers as sensors was proposed and demonstrated theoretically by introducing a thin  $\text{Al}_2\text{O}_3$  layer above the utmost Ag grating layer. We theoretically and numerically study the influence of the  $\text{Al}_2\text{O}_3$  layer on the plasmonic absorbers. The resonant wavelength of the sensor is easily tunable via geometrical scaling of the Ag grate structure and thickness of the  $\text{Al}_2\text{O}_3$  layer. The introduced  $\text{Al}_2\text{O}_3$  layer does not influence the underlying mechanism of the ultra-narrow absorber, so it remains the high sensitivity of the Ag-based plasmonic absorbers by keeping the sensitivity 507 nm/RIU and FOM about 160. The introduced anti-oxidized layer is an effective and harmless anti-oxidized strategy, which has great potential to improve the performance of sensors in practical applications.

**Keywords** Anti-oxidized strategy · Plasmonic sensor · Perfect absorbers

## 1 Introduction

Plasmonic sensors are sensitive to the refractive index change, which can detect small concentration of the molecule due to the surface plasmon resonance (SPR) mechanism (Lal et al. 2007; Anker et al. 2008; Guo et al. 2013; Miao et al. 2015; Ahmadian et al. 2013; Azzam et al. 2016; Kim et al. 2016). Metal nano-particles with different shapes were usually used to be the plasmonic sensors by localized SPR (Anker et al. 2008; Becker et al.

---

This article is part of the Topical Collection on Numerical Simulation of Optoelectronic Devices 2016.

Guest edited by Yuh-Renn Wu, Weida Hu, Slawomir Sujecki, Silvano Donati, Matthias Auf der Maur and Mohamed Swillam.

---

✉ Yulian Li  
ylli@shmtu.edu.cn

<sup>1</sup> College of Information Engineering, Shanghai Maritime University, Shanghai 201306, China

2010; Stewart et al. 2008; Qiu and Hu 2015). Recent advances show that more complex plasmonic sensors have also been explored, such as the electromagnetically induced transparency (Liu et al. 2010, 2009) and the plasmonic absorbers (Meng et al. 2014; Li et al. 2015b; Liu et al. 2015). Especially, the plasmonic absorbers show powerful ability to be sensors due to the near unity and controllable absorption characteristics (Li et al. 2015b).

The sensitivity of the plasmonic sensors can be improved through narrowing the resonance band and enhancing the resonance intensity (Becker et al. 2010). For the plasmonic absorbers, it is rather challenging to realize ultra-narrow absorption bands due to inherent large optical losses in metals, which decreases the quality factor of optical resonators (Li et al. 2014). Recent advances on the plasmonic absorbers show that it is amazing to use Ag for realizing ultra-narrow band plasmonic absorbers (Li et al. 2014, 2015b; Liu et al. 2015; Zhao et al. 2014; Chen et al. 2013b). However, the oxidized problem of the Ag material still influences the stability and working life of the Ag-based plasmonic sensors, which puts a limit on the practice application of the Ag-based plasmonic absorbers. Recent developments on the thin film deposition show powerful ability to anti-oxidization realization. Particularly, the atom layer deposition (ALD) method has shown great ability on the tuning plasmonic area (Zhang et al. 2014a, b; Chen et al. 2013a; Ciraci et al. 2014), which can control the thin film thickness at the Ångstrom using sequential, self-limiting surface reactions (George 2009).

In this paper, we propose and theoretically demonstrate an effective strategy to avoid the Ag oxidized problem of the plasmonic absorbers by introducing a thin  $\text{Al}_2\text{O}_3$  layer above the upmost Ag grating, which does not influence the high sensitivity of the plasmonic absorbers simultaneously. The thin  $\text{Al}_2\text{O}_3$  layer can be deposited accurately and conformally by ALD at the Ångstrom level. Furthermore, the resonant wavelength is easily tunable via geometrical scaling of the Ag grate structure and thickness of the  $\text{Al}_2\text{O}_3$  layer. The plasmonic absorber is ultrasensitive to the refractive index of the environmental dielectric with its FWHM as narrow as 3.2 nm and the FOM as high as 163. Introducing such thin  $\text{Al}_2\text{O}_3$  layer on the Ag grating surface is a promising route for avoiding the oxidized problem and achieving ultra-narrow band high sensitivity absorbers, which can immensely promote the practical application of sensors based on plasmonic absorbers. It may also be extended to be used in the area of absorption filters or narrow thermal emitters.

## 2 Numerical investigation

The plasmonic absorber is based on one-dimensional Ag grating constructed on a silver film, which is an old structure but still a hot topic today (Li et al. 2015b; Laroche et al. 2005; Popov et al. 2008; Sharon et al. 1997; Kravets et al. 2008; Hu et al. 2013; Liao and Zhao 2015). In order to avoid the Ag oxidized problem, we introduce a thin  $\text{Al}_2\text{O}_3$  layer above the upmost Ag surface with its thickness as  $d$  as illustrated in Fig. 1a, which presents the schematic diagram's cross section of a unit cell of the plasmonic absorber. The grey region is silver and the blue region is  $\text{Al}_2\text{O}_3$ . The height and the width of the Ag grating ridges are denoted as  $t$  and  $w$ , respectively. The thickness of the Ag film is denoted by  $h$  and the lattice constant is assumed to be  $a$ .

The spectral characteristics of the plasmonic absorbers are calculated by performing electromagnetic wave finite difference time domain method (FDTD, available from Lumerical software package) (Lumerical FDTD Solutions). A plane wave light source is

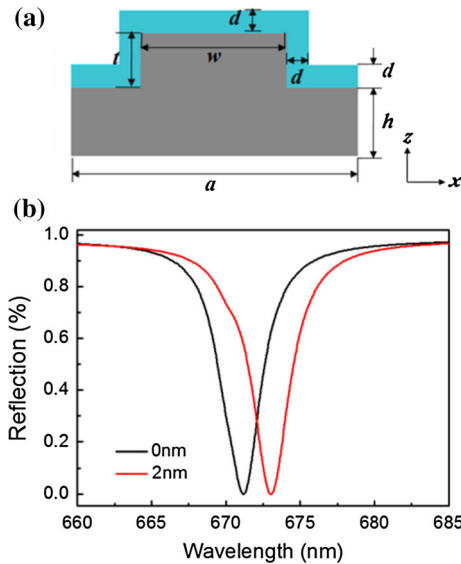


**Fig. 1** **a** The cross section of a unit cell of the plasmonic absorber. The *grey region* is silver and the *blue region* is  $\text{Al}_2\text{O}_3$ . The thickness of the thin  $\text{Al}_2\text{O}_3$  layer is denoted as  $d$ . The height and the width of the grating ridges are denoted as  $t$  and  $w$ , respectively. The thickness of the Ag film is denoted by  $h$  and the lattice constant is assumed to be  $a$ . A plane wave light source is used for illumination with its propagation direction and polarization along the negative  $z$ -axis and  $x$ -axis, respectively. **b** The reflection spectrum for the plasmonic absorber with  $d = 0$  or 2 nm, shown in the *black* and the *red line*, respectively. The other parameters are set as follows:  $a = 500$  nm,  $w = 100$  nm,  $t = 28$  nm and  $h = 100$  nm. (Color figure online)

used for illumination with its propagation direction and polarization along the negative  $z$ -axis and  $x$ -axis, respectively, as indicated in Fig. 1a. The permittivity of Ag is extracted from Johnson and Christy's work (Johnson and Christy 1972) in 1972 and simulated by Drude mode (Hao et al. 2011). The refractive index of  $\text{Al}_2\text{O}_3$  is 1.75. All materials are assumed to be nonmagnetic (i.e.,  $\mu = \mu_0$ ). The absorption spectrum ( $A$ ) of the device is retrieved from scattering parameters as follows:  $A = 1 - T - R$ , where  $A$ ,  $R$  and  $T$  denotes the absorption, reflection and transmission, respectively. In this work, the optically thick (100 nm) bottom silver film prevents the light transmission ( $T = 0$ ) and therefore the absorbance is  $A = 1 - R$ .

In Fig. 1b, the reflectance spectrums are plotted for the structure with the parameters as follows:  $a = 500$  nm,  $w = 100$  nm,  $t = 28$  nm,  $h = 100$  nm and  $d = 0$  nm or 2 nm. An extremely suppressed reflection dip is observed at the wavelength 671.1 nm with the maximum absorption over 99% at  $d = 0$  nm, which is shown in Fig. 1b in the black line. The bandwidth, the full width at half maximum (FWHM), is 3 nm. As the thickness of  $\text{Al}_2\text{O}_3$   $d = 2$  nm, the maximum absorption remains near unity and the FWHM maintains at 3 nm, while the absorption peak redshifts to 673 nm, as shown in Fig. 1b in the red line.

Now we study the optical properties of the absorber under different structural parameters and acquire the optimal structure. Figure 2a shows the reflection spectrum evolution of plasmonic absorbers as the height of grating ridge  $t$  increasing with  $w = 100$  nm and  $d = 2$  nm. When  $t$  increases from 10 to 100 nm, the absorption peaks show a continuous blue-shift and the intensity of the absorption peaks increase at first and then reduce. The biggest absorption peak intensity occurs as  $d$  is 28 nm. We find that the absorption peaks stay over 97% across a wide  $d$  range from 24 to 40 nm. Figure 2b shows the reflection

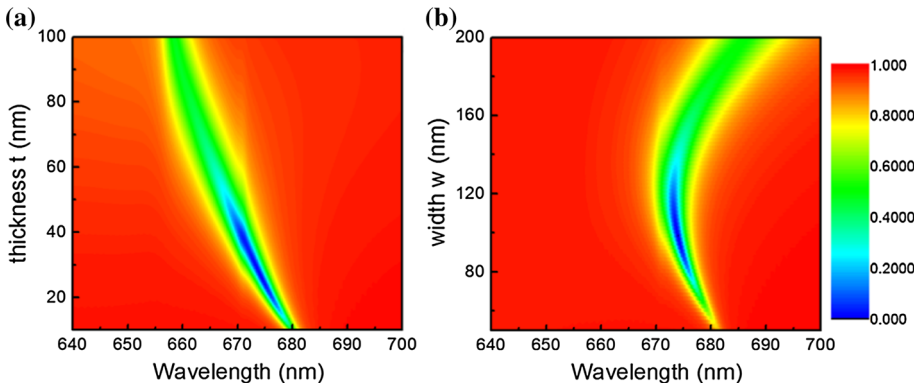


**Fig. 2** The reflection spectrum as the functions of the Ag grating ridge **a** thickness  $t$  varying from 10 to 100 nm with  $w$  invariant and **b** width  $w$  varying from 50 to 200 nm with  $t$  invariant

spectrum evolution of plasmonic absorbers versus the width of grating ridge  $w$ . As  $w$  increases from 50 to 200 nm, the absorption peaks blue-shift first and then red-shift with the intensity increasing at first and then reducing. The biggest absorption peak intensity occurs as  $w$  is 100 nm. The absorption peak intensity remains over 97% across a wide  $w$  range from 94 nm to 114 nm. The performance of the plasmonic absorbers is insensitive to the height  $t$  and width  $w$  of grating ridge, which makes the fabrication of the above optimized plasmonic absorbers easily. Furthermore the optimal performance occurs at the parameters  $t = 28$  nm and  $w = 100$  nm.

To reveal the mechanism of the unchanged near-unity sharp absorption peak after adding the  $\text{Al}_2\text{O}_3$  dielectric layer on the Ag grating structure, the normalized electric field intensity and normalized magnetic field distribution were extracted from the simulated peaks on the  $x$ - $z$  plane of the plasmonic absorbers with the thickness of the  $\text{Al}_2\text{O}_3$  layer 2 nm, as shown in Fig. 3a, b, respectively. The magnetic intensity distribution shown in Fig. 3b is paralleling the Ag grating. The calculated electric field intensity distribution pattern indicates that the highest absorb power intensity is located along the grating in the groove, which is due to interactions of strong diffraction and excited surface plasmon polaritons (SPP) at resonance wavelength (Le Perchec et al. 2008; Zayats et al. 2005). Under light incidence, the excited SPP wave is partially dissipated in metal as resistive heat described by resistive damping rate  $\gamma_{res}$ , and the other is radiated into free

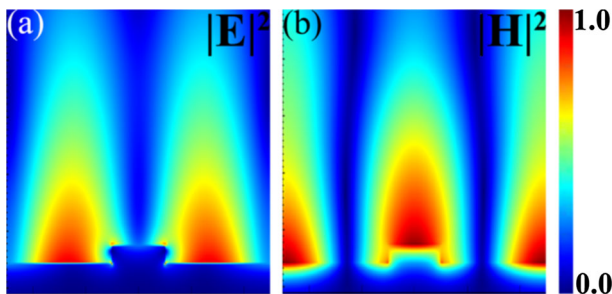


**Fig. 3** **a** The electric field intensity distribution and **b** the magnetic field intensity distribution from the resonant absorption peak on the  $x$ - $z$  plane of the plasmonic absorber with 2 nm  $\text{Al}_2\text{O}_3$  layer in thickness

space denoted by radiative damping rate  $\gamma_{rad}$ . For grating resonant systems, maximum absorption of electromagnetic waves occurs at the condition of critical coupling (Sharon et al. 1997; Yoon et al. 2010; Kurihara et al. 2002; Bliokh et al. 2006; Fan et al. 2003). At critical coupling condition, the resistive damping rate  $\gamma_{res}$  equals the radiative damping rate  $\gamma_{rad}$ . In Fig. 3a, b, the excited SPP field is distributed above the grating with a very slow decay and only a little electromagnetic field penetrates into the metal, which indicates that the resistive damping rate  $\gamma_{res}$  is small. So at the absorption peaks, the total damping rate under critical coupling condition is ultra-small, that is  $\gamma_{tot} = \gamma_{res} + \gamma_{rad} = 2\gamma_{res}$ , resulting in ultra-narrow band light dissipation of the near unity absorber. The electric field intensity distribution in Fig. 3a is similar with the electric field intensity distribution without  $\text{Al}_2\text{O}_3$  layer, which indicates that the  $\text{Al}_2\text{O}_3$  anti-oxidized layer does not affect the absorption mechanism of the plasmonic absorbers.

Here we study the performance of the plasmonic absorbers at various  $\text{Al}_2\text{O}_3$  layer thicknesses while the refractive index of the surround environment changes from 1.312 to 1.32. Figure 4a presents the reflection spectra with the thickness of the  $\text{Al}_2\text{O}_3$   $d$  varying from 0 to 5 nm with a step of 1 nm at  $n = 1.312$ . At  $n = 1.32$ , the spectrum is similar, so we do not show it here. As  $d$  varies, the maximum absorption intensity stays over 99% and FWHMs remain 3 nm too, which verify that the thickness of  $\text{Al}_2\text{O}_3$  layer almost does not influence the absorption intensity and FWHMs, but affects the peak position of the plasmonic absorber. As  $d$  increasing, the resonant peak wavelength redshifts. The redshift is due to extra phase shift from the  $\text{Al}_2\text{O}_3$  layer, and has a linear correlation with the thickness of  $\text{Al}_2\text{O}_3$  layer, as shown in Fig. 4b.

The resonant wavelength difference  $d\lambda$  between  $n = 1.312$  and  $1.32$  declines from 4.08 to 3.92 nm, down about 4%. Figure 4b reveals the FOM of the plasmonic absorbers decreases from 169 at  $d = 0$  nm to 157.4 at  $d = 5$  nm, falling about 6.8%, which is almost unchanged and still has a wonderful value. The value of FOM indicates that the performance of the plasmonic absorber is insensitivity to the thickness of the  $\text{Al}_2\text{O}_3$  layer.

For nano-metallic structure, resonant wavelength depends on the refractive index of the environmental dielectric, which is utilized to evaluate the performance of different types of plasmonic absorbers. The FWHM is another factor determining the performance of plasmonic sensors. Thus an overall performance parameter of the plasmonic sensor is defined as sensitivity ( $S = d\lambda/dn$ ) and figure of merit (FOM),  $\text{FOM} = d\lambda/dn/\text{FWHM}$ , introduced

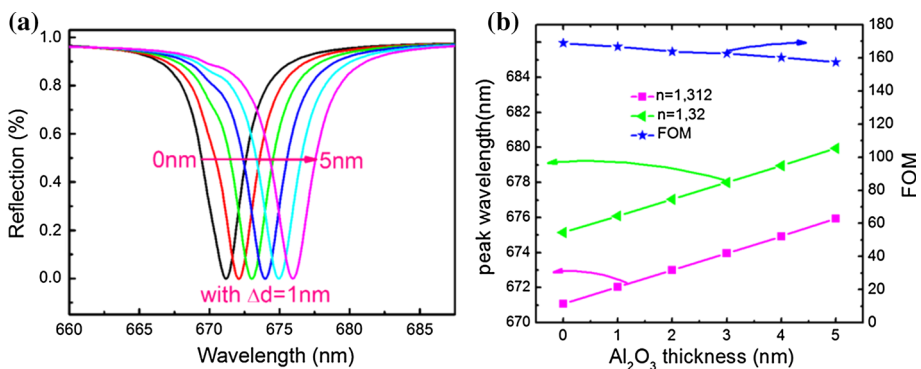


**Fig. 4** **a** The reflection spectra as the functions of the thickness of the anti-oxidized  $\text{Al}_2\text{O}_3$  layer varying from 0 to 5 nm. **b** The resonant peak wavelength at  $n = 1.312$  and  $n = 1.32$ , and the parameters FOM ( $\text{FOM} = \text{Max}d\lambda/dn/\text{FWHM}$ ) of the plasmonic absorber as the functions of the thickness of the  $\text{Al}_2\text{O}_3$  layer

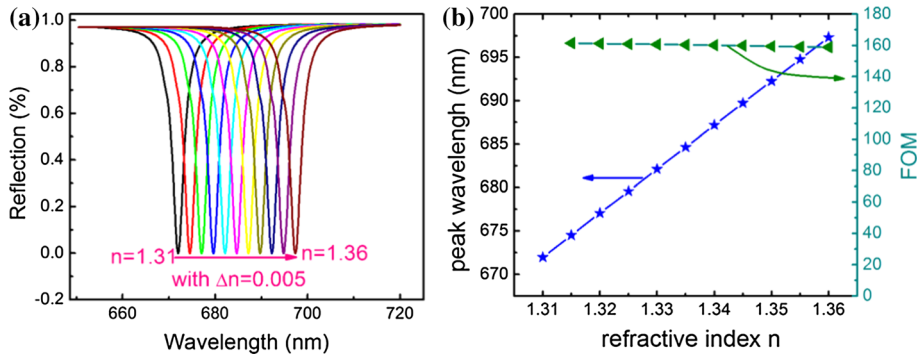


**Fig. 5** **a** The reflection spectra as the functions of the refractive index of the environmental dielectric varying from 1.31 to 1.36; **b** The resonant peak wavelength and FOM ( $\text{FOM} = \text{Max}|\text{d}\lambda/\text{d}n|/\text{FWHM}$ ) of the plasmonic absorber as the functions of the refractive index of the environmental dielectric varying from 1.31 to 1.36 in the *blue star* and *green triangle*, respectively. (Color figure online)

by (Becker et al. 2010), where  $\text{d}\lambda$  is resonant wavelength shift,  $\text{d}n$  is the refractive index change and FWHM is the full width of the half maximum at the absorption peak. Under normal incidence, the dependence of absorption spectra on the refractive index of the environmental dielectric  $n$  is shown in Fig. 5a with the structure parameters set as follows:  $a = 500$  nm,  $w = 100$  nm,  $t = 28$  nm,  $h = 100$  nm and  $d = 2$  nm. As  $n$  varies, the maximum absorption intensity remains near unity and FWHMs stay at 3 nm. At the same time, the resonant wavelength increases linearly as presented in Fig. 5a in the blue star. So according to the definition of  $S$  and FOM, the sensitivity and FOM of the plasmonic absorbers remain unchanged, which is about 507 nm/RIU and 160, respectively. Figure 5b shows the  $S$  in the slope of the blue star and the FOM in the green triangle. The characterized wavelength in our work mainly focuses on the visible region which is compatible to the current data of the plasmonic sensor (Meng et al. 2014; Tong et al. 2014; Li et al. 2015a), only being less than some of them (Meng et al. 2014). Thus, the plasmonic absorber has an excellent performance for detecting the refractive index fluctuation of the surround environment after introducing the  $\text{Al}_2\text{O}_3$  layer.

### 3 Conclusion

In summary, we proposed an effective strategy to avoid the oxidization of the Ag based plasmonic absorbers by introducing a thin  $\text{Al}_2\text{O}_3$  layer above the upmost Ag surface and achieve an ultra-narrow band highly sensitive sensor, simultaneously. The interaction of strong diffraction and excited SPP at resonance wavelength is proposed to explain the near unity absorbance. The expected perfect absorption (100% absorbance), narrow FWHM about 3 nm, high sensitivity about 507 nm/RIU, and high FOM about 160 are achieved. They are independent of the thickness of the introduced  $\text{Al}_2\text{O}_3$  layer and the refractive index fluctuation of the surround environment, which makes the sensor stable working at various environments. This work may greatly promote the practical application of sensors based on plasmonic absorbers.

**Acknowledgements** The authors thank Jun Yin for helpful discussion and technical supporting. This work was funded by National Natural Science Foundation of China (Nos. 61504078), China Postdoctoral Science Foundation (Nos. 2015M571545) and National Natural Science Foundation of China (Nos. 61303099).

## References

- Ahmadian, D., Ghobadi, C., Nourinia, J.: Ultra-compact two-dimensional plasmonic nano-ring antenna array for sensing applications. *Opt. Quant. Electron.* **46**(9), 1097–1106 (2013)
- Anker, J.N., Hall, W.P., Lyandres, O., Shah, N.C., Zhao, J., Van Duyne, R.P.: Biosensing with plasmonic nanosensors. *Nat. Mater.* **7**(6), 442–453 (2008)
- Azzam, S.I., Hameed, M.F.O., Shehata, R.E.A., Heikal, A.M., Obayya, S.S.A.: Multichannel photonic crystal fiber surface plasmon resonance based sensor. *Opt. Quant. Electron.* **48**(2), 142 (2016)
- Becker, J., Trugler, A., Jakab, A., Hohenester, U., Sonnichsen, C.: The optimal aspect ratio of gold nanorods for plasmonic bio-sensing. *Plasmonics* **5**(2), 161–167 (2010)
- Bliokh, K.Y., Bliokh, Y.P., Freilikher, V., Genack, A.Z., Hu, B., Sebbah, P.: Localized modes in open one-dimensional dissipative random systems. *Phys. Rev. Lett.* **97**(24), 243904 (2006)
- Chen, X., Park, H., Pelton, M., Piao, X., Lindquist, N.C., Im, H., Kim, Y.J., Ahn, J.S., Ahn, K.J., Park, N., Kim, D., Oh, S.: Atomic layer lithography of wafer-scale nanogap arrays for extreme confinement of electromagnetic waves. *Nat. Commun.* **4**, 2361 (2013a)
- Chen, Z., Wang, C., Wang, L., Jiang, C., Zhu, H.: Surface plasmonic resonance sensor by metal strip pair arrays. *Opt. Quant. Electron.* **45**(7), 707–712 (2013b)
- Ciraci, C., Chen, X., Mock, J.J., McGuire, F., Liu, X., Oh, S.-H., Smith, D.R.: Film-coupled nanoparticles by atomic layer deposition: comparison with organic spacing layers. *Appl. Phys. Lett.* **104**(2), 023109 (2014)
- Fan, S., Suh, W., Joannopoulos, J.D.: “Temporal coupled-mode theory for the fano resonance in optical resonators”. *J. Opt. Soc. Am. A*: **20**(3), 569–572 (2003)
- George, S.M.: Atomic layer deposition: an overview. *Chem. Rev.* **110**(1), 111–131 (2009)
- Guo, N., Hu, W., Chen, X., Wang, L., Lu, W.: Enhanced plasmonic resonant excitation in a grating gated field-effect transistor with supplemental gates. *Opt. Expr.* **21**(2), 1606–1614 (2013)
- Hao, J., Zhou, L., Qiu, M.: Nearly total absorption of light and heat generation by plasmonic metamaterials. *Phys. Rev. B* **83**(16), 165107 (2011)
- Hu, W.D., Wang, L., Chen, X.S., Guo, N., Miao, J.S., Yu, A.Q., Lu, W.: Room-temperature plasmonic resonant absorption for grating-gate GaN HEMTs in far infrared terahertz domain. *Opt. Quant. Electron.* **45**(7), 713–720 (2013)
- Johnson, P.B., Christy, R.W.: Optical constants of the noble metals. *Phys. Rev. B* **6**(12), 4370–4379 (1972)
- Kim, H.-S., Kumar, M.D., Kim, H., Kim, J.: Increased spectral sensitivity of Si photodetector by surface plasmon effect of Ag nanowires. *Infrared Phys. Technol.* **76**, 621–625 (2016)
- Kravets, V.G., Schedin, F., Grigorenko, A.N.: Plasmonic blackbody: almost complete absorption of light in nanostructured metallic coatings. *Phys. Rev. B* **78**(20), 205405 (2008)
- Kurihara, K., Suzuki, K.: Theoretical understanding of an absorption-based surface plasmon resonance sensor based on Kretschmann’s theory. *Anal. Chem.* **47**(3), 696–701 (2002)
- Lal, S., Link, S., Halas, N.J.: Nano-optics from sensing to waveguiding. *Nat. Photon.* **1**(11), 641–648 (2007)
- Laroche, M., Arnold, C., Marquier, F., Carminati, R., Greffet, J.J., Collin, S., Bardou, N., Pelouard, J.L.: Highly directional radiation generated by a tungsten thermal source. *Opt. Lett.* **30**(19), 2623 (2005)
- Le Perchec, J., Quémerais, P., Barbara, A., López-Ríos, T.: Why metallic surfaces with grooves a few nanometers deep and wide may strongly absorb visible light. *Phys. Rev. Lett.* **100**(6), 066408 (2008)
- Li, G., Shen, Y., Xiao, G., Jin, C.: Double-layered metal grating for high-performance refractive index sensing. *Opt. Expr.* **23**(7), 8995–9003 (2015a)
- Li, Y., An, B., Jiang, S., Gao, J., Chen, Y., Pan, S.: Plasmonic induced triple-band absorber for sensor application. *Opt. Expr.* **23**(13), 17607–17612 (2015b)
- Li, Z., Butun, S., Aydin, K.: Ultranarrow band absorbers based on surface lattice resonances in nanostructured metal surfaces. *ACS Nano* **8**(8), 8242–8248 (2014)
- Liao, Y.-L., Zhao, Y.: A wide-angle TE-polarization absorber based on a bilayer grating. *Opt. Quant. Electron.* **47**(8), 2533–2539 (2015)
- Liu, N., Langguth, L., Weiss, T., Kastel, J., Fleischhauer, M., Pfau, T., Giessen, H.: Plasmonic analogue of electromagnetically induced transparency at the drude damping limit. *Nat. Mater.* **8**(9), 758–762 (2009)
- Liu, N., Weiss, T., Mesch, M., Langguth, L., Eigenthaler, U., Hirscher, M., Soennichsen, C., Giessen, H.: Planar metamaterial analogue of electromagnetically induced transparency for plasmonic sensing. *Nano Lett.* **10**(4), 1103–1107 (2010)
- Liu, Z., Liu, G., Huang, S., Liu, X., Wang, Y., Liu, M., Gu, G.: Enabling access to the confined optical field to achieve high-quality plasmon sensing. *IEEE Photonic. Tech. L.* **27**(11), 1212–1215 (2015)
- Meng, L., Zhao, D., Ruan, Z., Li, Q., Yang, Y., Qiu, M.: Optimized grating as an ultra-narrow band absorber or plasmonic sensor. *Opt. Lett.* **39**(5), 1137–1140 (2014)

- Miao, J., Hu, W., Jing, Y., Luo, W., Liao, L., Pan, A., Wu, S., Cheng, J., Chen, X., Lu, W.: Surface plasmon-enhanced photodetection in few layer MoS<sub>2</sub> phototransistors with Au nanostructure arrays. *Small* **11**(20), 2392–2398 (2015)
- Popov, E., Maestre, D., McPhedran, R.C., Nevière, M., Hutley, M.C., Derrick, G.H.: Total absorption of unpolarized light by crossed gratings. *Opt. Expr.* **16**(9), 6146–6155 (2008)
- Qiu, W., Hu, W.: Laser beam induced current microscopy and photocurrent mapping for junction characterization of infrared photodetectors. *Sci. China Phys. Mech. Astron.* **58**(2), 1–13 (2015)
- Sharon, A., Glasberg, S., Rosenblatt, D., Friesem, A.A.: Metal-based resonant grating waveguide structures. *J. Opt. Soc. Am. A*: **14**(3), 588–595 (1997)
- Stewart, M.E., Anderton, C.R., Thompson, L.B., Maria, J., Gray, S.K., Rogers, J.A., Nuzzo, R.G.: Nanostructured plasmonic sensors. *Chem. Rev.* **108**(2), 494–521 (2008)
- Tong, L., Wei, H., Zhang, S., Xu, H.: Recent advances in plasmonic sensors. *Sensors* **14**(5), 7959–7973 (2014)
- Yoon, J., Seol, K.H., Song, S.H., Magnusson, R.: Critical coupling in dissipative surface-plasmon resonators with multiple ports. *Opt. Express* **18**(25), 25702–25711 (2010)
- Zayats, A.V., Smolyaninov, I.I., Maradudin, A.A.: Nano-optics of surface plasmon polaritons. *Phys. Rep.* **408**(3–4), 131–314 (2005)
- Zhang, Y., Wei, T., Dong, W., Zhang, K., Sun, Y., Chen, X., Dai, N.: Vapor-deposited amorphous meta-materials as visible near-perfect absorbers with random non-prefabricated metal nanoparticles. *Sci. Rep.* **4**, 4850 (2014a)
- Zhang, Y., Zhang, K., Zhang, T., Sun, Y., Chen, X., Dai, N.: Distinguishing plasmonic absorption modes by virtue of inversed architectures with tunable atomic-layer-deposited spacer layer. *Nanotechnology* **25**(50), 504004 (2014b)
- Zhao, D., Meng, L., Gong, H., Chen, X., Chen, Y., Yan, M., Li, Q., Qiu, M.: Ultra-narrow-band light dissipation by a stack of lamellar silver and alumina. *Appl. Phys. Lett.* **104**(22), 221107 (2014)